

Compatibility and cytotoxicity of poly(ϵ -caprolactone)/polypyrrole-block-poly(ϵ -caprolactone) blend films in fibroblast bovine cells

Nelson Luis Gonçalves Dias de Souza^{1,2*} , Grasielle Soares Cavallini^{1,2} , Tiago Teixeira Alves² , Michele Munk Pereira³ , Humberto de Mello Brandão⁴  and Luiz Fernando Cappa de Oliveira⁵ 

¹*Colegiado de Ciências Exatas e Biotecnológicas, Universidade Federal do Tocantins – UFT, Gurupi, TO, Brasil*

²*Programa de Pós-graduação em Química, Universidade Federal do Tocantins – UFT, Gurupi, TO, Brasil*

³*Departamento de Biologia, Instituto de Ciências Biológicas, Universidade Federal de Juiz de Fora – UFJF, Juiz de Fora, MG, Brasil*

⁴*Empresa Brasileira de Pesquisa Agropecuária – Embrapa Gado de Leite, Juiz de Fora, MG, Brasil*

⁵*Núcleo de Espectroscopia e Estrutura Molecular, Departamento de Química, Universidade Federal de Juiz de Fora – UFJF, Juiz de Fora, MG, Brasil*

*nelson.luis@uft.edu.br

Abstract

Polymer blends, derived from the combination of two or more polymers, yield novel materials with properties distinct from that of the original polymers. These materials have garnered interest in the medical field. However, for such applications the biocompatibility of the material must be evaluated. In this study, we prepared polymer blends from poly(ϵ -caprolactone) (PCL) and polypyrrole-block-poly(ϵ -caprolactone) (PPy-*b*-PCL) using the casting method. The observed compatibility resulted from specific interactions between the carboxylic group of PCL and the amine group of PPy-*b*-PCL, as well as between the pyrrole ring of PPy-*b*-PCL and the CH₂ group of PCL. Micro-Raman imaging revealed homogeneity in surface morphology, whereas thermogravimetric analysis indicated that the formation of polymer blends enhances the material's thermal stability. Importantly, the results demonstrated that the addition of PPy-*b*-PCL does not affect the cytotoxicity to bovine fibroblasts, suggesting their biocompatibility and potential application in cattle veterinary devices.

Keywords: *biocompatibility, cell proliferation, polymer blends.*

How to cite: Souza, N. L. G. D., Cavallini, G. S., Alves, T. T., Pereira, M. M., Brandão, H. M., & Oliveira, L. F. C. (2024). Compatibility and cytotoxicity of poly(ϵ -caprolactone)/polypyrrole-block-poly(ϵ -caprolactone) blend films in fibroblast bovine cells. *Polímeros: Ciência e Tecnologia*, 34(1), e20240007. <https://doi.org/10.1590/0104-1428.20230082>

1. Introduction

Polymer blends are created by combining two or more polymers to yield a new material with properties distinct from that of the original polymers^[1,2]. The fabrication of these blends is a cost-effective method for generating new polymer materials, as it eliminates the need to synthesize new polymers^[3]. During the production of a blend, two factors must be considered: miscibility and compatibility. Thermodynamically miscible polymers intermingle at the molecular level, a process that should result in negative Gibbs free energy. The final properties of miscible blends typically represent an average of the properties of the blend components. Conversely, immiscible mixtures form a heterogeneous system, where the properties of the constituent components are retained^[4]. The term compatibility, however, has various interpretations in the literature. Some authors describe compatible polymers as those that do not show significant phase separation upon mixing or when the desired physical properties are attained^[5]. A definition of compatibility suggested by Coleman and Painter involves

the application of infrared spectroscopy. Accordingly, if two polymers are compatible, the spectrum of the mixture should exhibit changes when contrasted with the spectra of the pure polymers^[6].

Polymeric systems have garnered significant interest in the medical field, finding applications in the development of controlled release systems, mucoadhesive films, bioseparation, vascular prostheses, hemodialysis membranes, urinary catheters, dressings, and orthopedic implants, among others^[7,8]. However, the biocompatibility of these materials must be evaluated before use. The in-vitro cytotoxicity assay serves as the initial test to determine the biocompatibility of any material intended for biomedical devices^[9].

The literature describes numerous cytotoxicity tests, most of which measure cell death or other detrimental effects on cell function. Consequently, if a material demonstrates inertness in cell culture under these test conditions, its potential for use in biomedical devices is enhanced^[10].

The primary cause of polymer cytotoxicity is the presence of charged functional groups within the polymer structure. These groups can interact with the cell membrane, potentially causing rupture, interfering with the transport of vital materials to the cell, or chelating essential cellular nutrients^[11].

Poly(ϵ -caprolactone) (PCL) is a biodegradable and bioabsorbable polymer that has gained attention due to its low cost. In realistic applications, PCL with a high molecular weight is preferred because it improves the mechanical properties resulting from the entanglement of the polymeric chains^[12]. This linear, semi-crystalline synthetic polyester possesses an orthorhombic crystalline structure and can be readily prepared through the catalytic polymerization of the caprolactone monomer. Its hydrophobic nature and high crystallinity ensures that it undergoes hydrolysis at a slow pace^[13,14]. Because of these interesting properties this polymer has been used alone and in combination with a range of materials in different types of biomedical applications^[15].

Conductive polymers are utilized in neural tissue engineering due to their superior electrical properties^[16]. Polypyrrole (PPy), in particular, has garnered significant attention in the medical field. This is attributed to its ease of synthesis, potential for chemical modifications, well-documented *in vitro* and *in vivo* biocompatibility, and relatively high conductivity under physiological conditions^[17-19]. However, PPy is not biodegradable, which is a desirable property for tissue engineering constructs. This makes it necessary to reduce its content to the lowest possible levels^[20,21]. In this context, some polymeric materials using PPy have been reported in literature. Hydrogels containing low concentrations of PPy promoted cell adhesion, growth, and neuronal differentiation of human bone marrow mesenchymal stem cells. Therefore, they may serve as a useful platform to study the effects of electrical and mechanical signals on these cells and to develop multifunctional scaffolds for neural tissue engineering^[22]. Collagen/PPy-*b*-PCL hydrogels containing 0.5, 1.0, and 2.0% PPy-*b*-PCL were developed and showed good printability and biocompatibility. Thus, they have the potential to be used in the bioprinting of neural tissue constructs, for the repair of damaged neural tissues, and drug testing or precision medicine applications^[23].

The aim of this study was to fabricate and characterize films of polymer blends composed of copolymer PPy-*b*-PCL (biodegradable and conductive polymer) and PCL. The analysis focused on assessing compatibility, supramolecular interactions, and potential cytotoxic effects on bovine fibroblasts.

2. Materials and Methods

2.1 Materials

The PCL (MW = 80,000 g.mol⁻¹), PPy-*b*-PCL (MW = PPy: 4,000 g.mol⁻¹ and PCL: 2,000 g.mol⁻¹), Dulbecco's Modified Eagle Medium-F12 (DMEM), fetal bovine serum (FBS) and penicillin-streptomycin antibiotics were procured from Sigma-Aldrich® (St. Louis, MO, USA) and used without further purification. Dichloromethane and ethanol, purchased from Vetec®, was employed as a solvent, also without further purification. The reference controls, high-density

polyethylene (HDPE) and polyurethane, which contained 0.1% zinc diethyldithiocarbamate (ZDEC), were obtained from the Food and Drug Safety Center (Kanagawa, Japan). Phosphate buffered saline (PBS) was purchased from LGC Biotechnology (São Paulo, Brazil).

2.2 Preparation of polymer blends

Polymer blends were prepared using the solvent evaporation technique. In this method, the selected polymers are dissolved in a specific solvent and the solution is stirred for a certain period of time to obtain a homogeneous solution. After the solvent had evaporated, the resulting product was collected^[24]. Thus, five distinct solutions (2.0% m/v) of PCL and PPy-*b*-PCL in dichloromethane were prepared by combining the polymers in weight ratios of 0/100, 1/99, 3/97, 5/95, and 100/0 for PPy-*b*-PCL and PCL, respectively (Table 1). The mass of PCL was calculated assuming a purity of 100%. However, since PPy-*b*-PCL is a dispersion with a purity range of 0.3-0.7%, we used a purity value of 0.7% to determine the mass of the solution needed to obtain the required amount of PPy-*b*-PCL for the polymer blend. These solutions were stirred (120 rpm) for approximately 24 hours before being transferred to Petri dishes to facilitate solvent evaporation at room temperature (26 °C). The blends were subsequently collected as cast films^[25,26].

2.3 Cytotoxicity test

Primary fibroblast cell cultures derived from bovine skin biopsies were acquired from the cell bank of the Laboratory of Animal Reproduction and Biotechnology of Brazilian Agricultural Research Corporation. The cells were cultured at 37 °C, 5% CO₂ and 95% humidity, in Dulbecco's modified Eagle's medium supplemented with 10% fetal calf serum and 100 units mL⁻¹ penicillin-streptomycin and were cryopreserved at the second passage. Prior to their utilization, fibroblasts were thawed and cultured until the third passage.

The direct contact assay was performed with a monolayer of bovine fibroblasts. Briefly, 4x10⁵ cells/well were seeded uniformly into six-well plates (35 mm diameter) and cultured for 48 h. Subsequently, polymer films (1.0 cm x 1.0 cm) were carefully placed at the center of the wells and incubated for 24 h. Following this, the films were removed, the culture medium was discarded, and the plates were washed with phosphatebuffered saline and stained with a solution of 0.2% crystal violet in ethanol for 20 min. The cytotoxicity of the polymer films was determined by observing the cells by phase contrast and by qualitative means, the zone index value (Table 2). This analysis was performed under an inverted light microscope (ICM 405, Zeiss, Germany) with a camera (AxioCam ERC 5 s, Zeiss, Germany) attached to a computer for the images to be captured.

Table 1. Polymer blend films composition and code.

Films	PPy- <i>b</i> -PCL (%)	PCL (%)
PCL	0.0	100.0
1 PPy- <i>b</i> -PCL/ 99 PCL	1.0	99.0
3 PPy- <i>b</i> -PCL/ 97 PCL	3.0	93.0
5 PPy- <i>b</i> -PCL/ 95 PCL	5.0	95.0
PPy- <i>b</i> -PCL	100.0	0.0

Image capture and the distance between viable cells and films were measured using Zen 2.3 lite software. For positive and negative controls, we used polyurethane containing 0.1% ZDEC (zinc diethyldithiocarbamate) and HDPE (high-density polyethylene), respectively^[27].

2.4 Vibrational spectroscopy

Fourier transform infrared (FTIR) spectra were obtained in an ALPHA FT-IR Bruker Spectrometer in the 4000-600 cm^{-1} region. For the samples, we used the method of attenuated total reflection (ATR), with a resolution of 2 cm^{-1} and 64 scan accumulations. Raman measurements were performed on a Bruker RFS 100 equipment excited with a Nd^{3+} /YAG laser operating at 1064 nm, equipped with a CCD detector cooled with liquid nitrogen and a spectral resolution of 2 cm^{-1} .

An average of 1024 scans were collected with a laser power of 50 mW directed at the sample.

2.5 Micro-Raman imaging

The measurements were performed on Bruker SENTERRA equipment attached to the microscope. The Raman image was acquired by mapping one hundred points of the sample using an optical lens 50 times, laser excitation at 785 nm, average 25 co-additions and 3 seconds of exposure for each point, a laser power of 10mW and spectral resolution of 4 cm^{-1} .

2.6 Thermogravimetric analysis

Thermogravimetric analyses (TGA) were performed in a Shimadzu TG-60 instrument under nitrogen atmosphere in a flow of 50.0 $\text{mL}\cdot\text{min}^{-1}$, with a heating rate of 10 $^{\circ}\text{C}\cdot\text{min}^{-1}$, from 25 to 600 $^{\circ}\text{C}$.

Table 2. Cytotoxicity index by reactivity grades classification.

Grade	Description of the reactive Zone	Cytotoxicity
0	No zone rises around the sample	Without
1	Limited under the sample area	Slightly
2	Zone not greater than 2 mm	Mildly
3	Zone between 2 and 10 mm	Moderately
4	Zone between 10 and 20 mm	Severely

3. Results and Discussions

The infrared and Raman spectra of the polymers are depicted in Figures 1 and 2, respectively, with tentative band assignments presented in Table 3, derived from a comparison with literature data^[10,28-35].

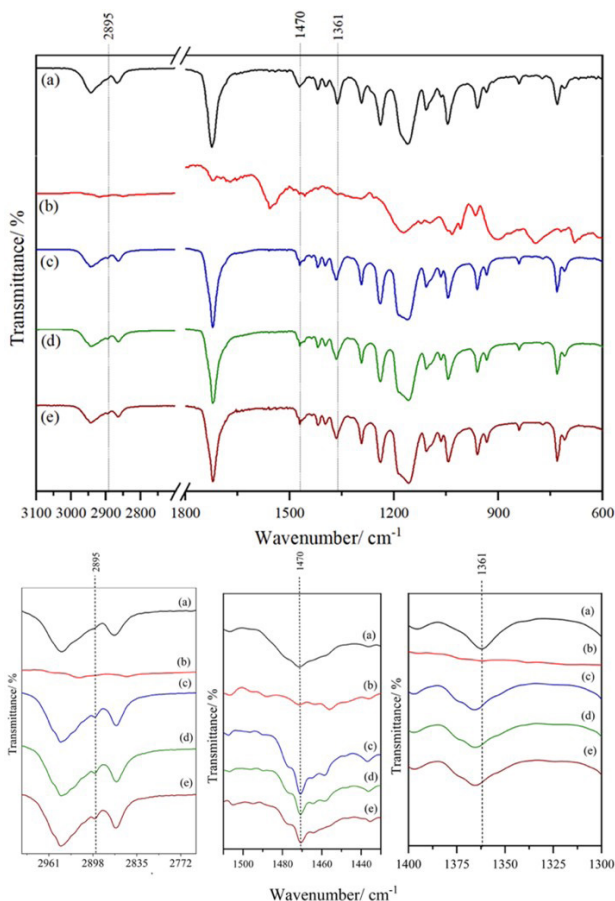


Figure 1. Infrared absorption spectra of PCL (a) PPy - b -PCL (b), 1 PPy - b -PCL/ 99 PCL (c), 3 PPy - b -PCL/ 97 PCL (d) and 5 PPy - b -PCL/ 95 PCL (e).

In the infrared spectra of polymer blends, the only discernible changes pertain to the bands associated with the C–H bond vibration. A new band at 2895 cm⁻¹ is observable in the polymer blend spectra, along with the narrowing of the band at 1470 cm⁻¹, emergence of shoulders at 1458 and 1463 cm⁻¹, and shift of the band at 1361 cm⁻¹ to 1365 cm⁻¹. The Raman spectrum of the 5 *PPy-b-PCL* / 95 PCL blend exhibits changes; the bands at 1587, 1237, and 936 cm⁻¹, associated with the polymer *PPy-b-PCL*, shift to larger wavenumbers, while the bands at 1722, 1441, and 1305 cm⁻¹, associated with the polymer PCL, shift to 1728, 1446, and 1310 cm⁻¹, respectively. Consequently, the vibrational spectroscopy data suggest the existence of two types of intermolecular interactions: hydrogen bonds between the carbonyl of PCL and the amine group of *PPy-b-PCL*, and CH– π type interaction between the *PPy-b-PCL* pyrrole ring and the CH₂ group of PCL (Figure 3). Studies on blends using PCL and PPy, a material similar to the one in this study, revealed the presence of hydrogen bonds in the polymeric mixtures and the absence of PPy domains in the mixtures due to this interaction. Furthermore, the formation of the polymer blend has led to enhanced physical and chemical properties^[36,37].

Heterogeneity often arises in the composition and morphology of polymer blends. In this context, it is believed that the general material properties generally depend to a large extent on the relevant microscopic heterogeneity. Therefore, to better understand the influence of heterogeneity on material properties, it is desirable to obtain sample information with high spatial resolution. Thus, micro-Raman image analysis can be used to study the spatial distribution of molecular species within polymer mixtures^[38]. Figure 4 shows the micro-Raman image of the polymer blends, focusing on the *PPy-b-PCL* band at 1588 cm⁻¹. This was chosen because it is a region in which only *PPy-b-PCL* shows a signal and because this component is present in a smaller proportion. In the Raman image of all the mixtures, 100 points were analysed and in all of them the presence

of bands at 1588 cm⁻¹ was observed, with more or less intensity, represented by blue to pink colouration on the contour map. This fact indicates the presence of *PCL-b-PPy* at all points of the sample and the non-heterogeneity at a spatial resolution of approximately 1mm^[39]. There are no studies in the literature on the morphology of blends formed between PCL and *PCL-b-PPy*. However, a study of the morphology of PCL/PPy blends (95/5, 90/10 and 85/15) showed that PPy is homogeneously distributed in the host matrix and does not show PPy agglomerates in isolated domains^[36].

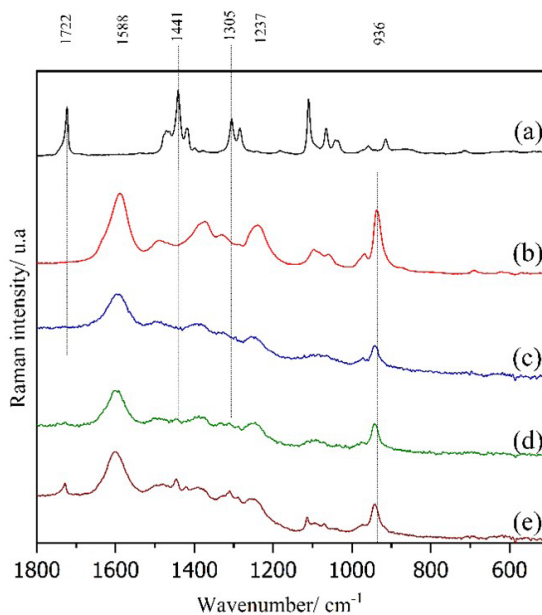


Figure 2. Raman spectra excited at 1064 nm of PCL (a), *PPy-b-PCL* (b), 1 *PPy-b-PCL* / 99 PCL (c), 3 *PPy-b-PCL* / 97 PCL (d) and 5 *PPy-b-PCL* / 95 PCL (e).

Table 3. Main infrared absorption and Raman wavenumber values (in cm⁻¹) of samples.

<i>PPy-b-PCL</i>		PCL		Tentative assignment
FTIR	Raman	FTIR	Raman	
		2942/2867	2919/2866	$\nu(\text{CH}_2)$
1720		1722	1722	$\nu(\text{C}=\text{O})$
1556	1587			$\nu(\text{C}=\text{C})$
		1470/1395/1361	1467/1441/1417	$\delta(\text{CH}_2)$
	1489/1380			$\nu(\text{C}-\text{N})$
1454/1170				vibration of the pyrrole ring
			1305/1284	$\omega(\text{CH})$
1257	1328	1290		$\nu(\text{C}-\text{C})$
	1237			$\delta(\text{NH})$
1031		1238/1107/1045	1110/1039	$\nu(\text{C}-\text{O}-\text{C})$
	1237/1097/1058/968		1061	$\delta(\text{CH})$
		1161		$\nu(\text{C}-\text{O})$
			913/957	$\nu(\text{C}-\text{COO})$
965		960/930		$\delta(\text{C}-\text{O}-\text{C})$
	936			pyrrole ring deformation
790				$\omega(\text{C}-\text{H})$

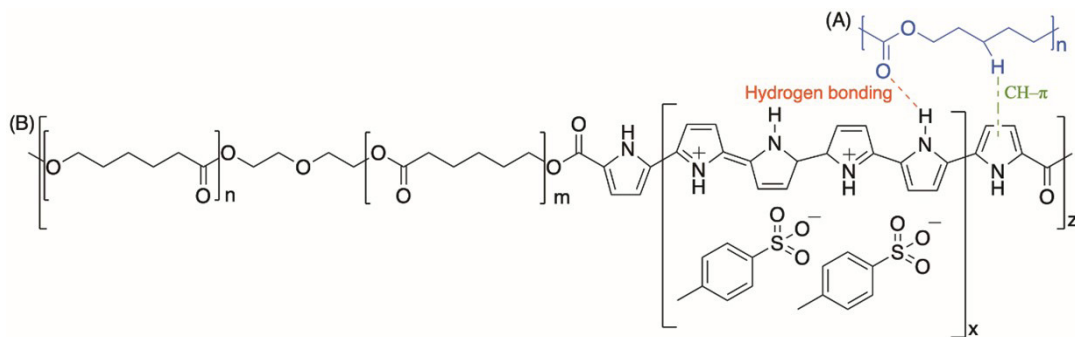


Figure 3. Illustration of CH- π and hydrogen bonding interactions between PCL (A) and PPy-b-PCL (B).

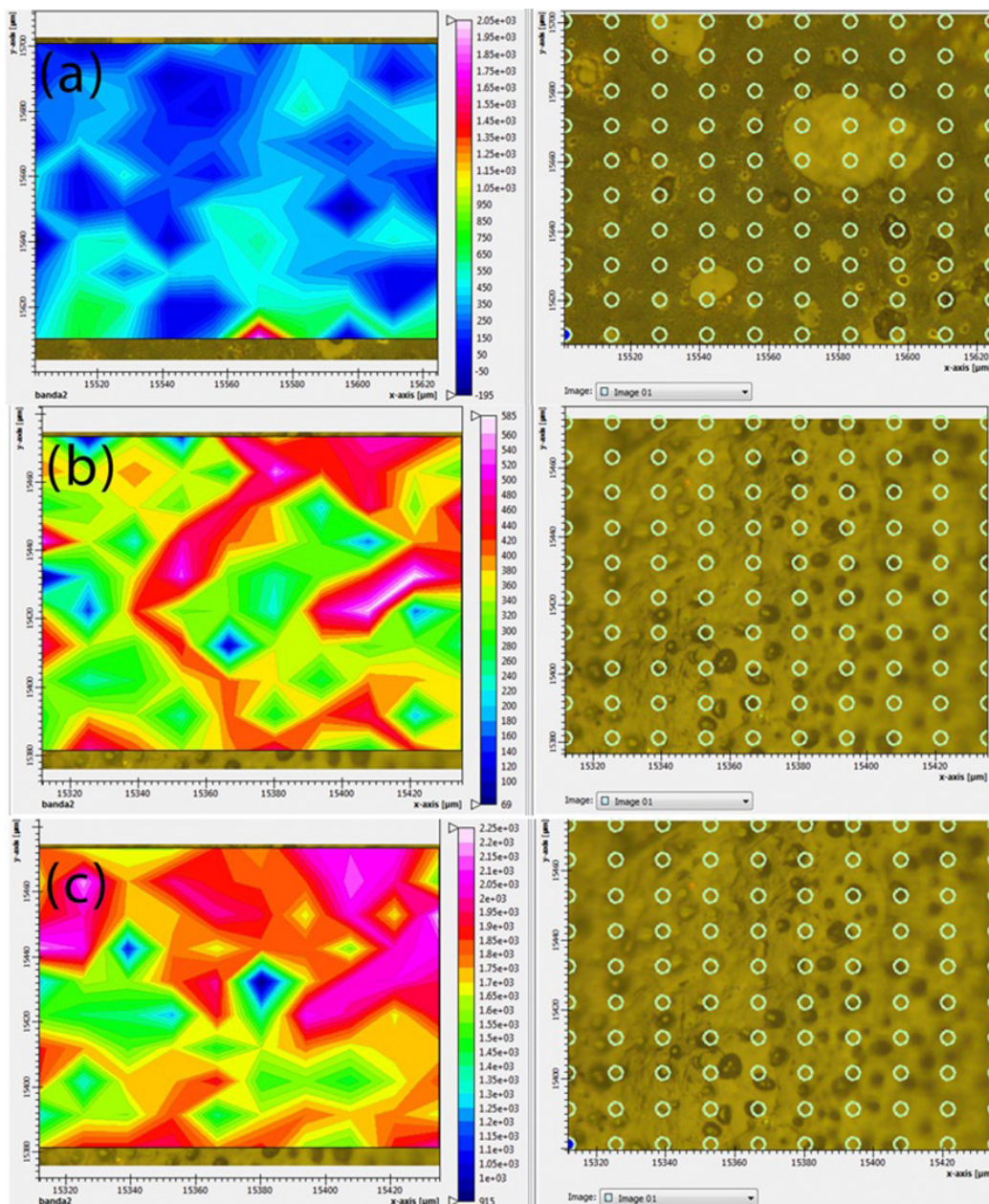


Figure 4. Micro-Raman Imaging of 1 PPy-b-PCL/ 99 PCL (a), 3 PPy-b-PCL/ 97 PCL (b) and 5 PPy-b-PCL/ 95 PCL (c).

Figure 5 depicts the TGA (Thermogravimetric analysis) and DTG (derivative thermogravimetry) curves, respectively, for PCL, *PPy-b-PCL*, and their blends, with corresponding thermal data provided in Table 4. The TGA curve for PCL exhibits a single decomposition step characteristic of this compound, related to random fission of the polymeric chain and subsequent formation of CO₂, H₂O, 5-hexenoic acid, and caprolactone^[40]. However, while PCL fully degrades at 550 °C, *PPy-b-PCL* experiences a 45% mass loss at the same temperature. The thermal data analysis for the polymer blends reveals their distinct behavior compared to that of the pure polymers. The T_{onset} temperature for all blends is very close to that of the polymer with the higher T_{onset} (PCL), which can be explained by the low concentration of *PPy-b-PCL* in the polymer films. In terms of DTG curve analysis, the Td_{max} temperature (maximum degradation rate temperature) for the polymer blends exceeds that of the PCL polymer. This increase in the maximum degradation temperature values may be related to the compatibility of

these two polymers and the presence of intermolecular interactions between them^[41-43].

Optical micrographs (Figure 6) demonstrate that the polymer films produced do not cause any morphological changes in the shape of the fibroblasts, which would indicate signs of cytotoxicity, in accordance with the morphological criteria established in the literature^[44,45].

Table 4. Thermal data of the samples.

Samples	TGA	DTG
	T _{onset} (°C)	Td _{max} (°C)
PCL	386	396
1 <i>PPy-b-PCL</i> / 99 PCL	383	408
3 <i>PPy-b-PCL</i> / 97 PCL	386	413
5 <i>PPy-b-PCL</i> / 95 PCL	382	409
<i>PPy-b-PCL</i>	207	238

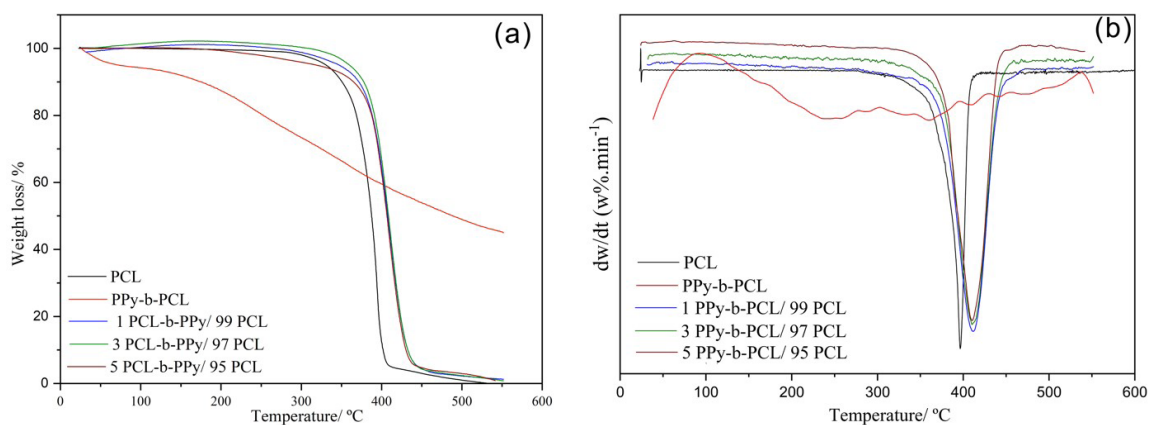


Figure 5. TGA (a) and DTG (b) curves of the samples.

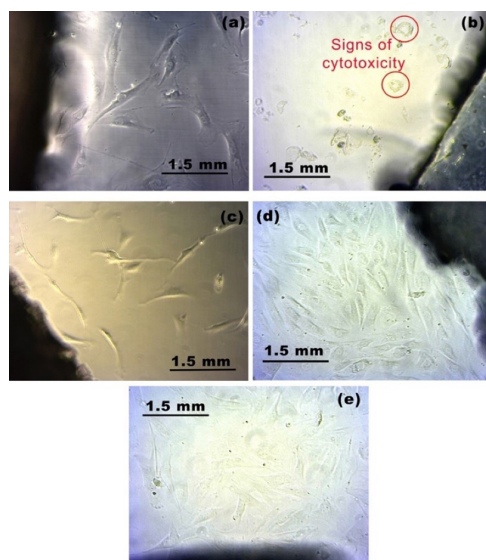


Figure 6. Inverted optical microscope images of negative control (a), positive control (b), 1 *PPy-b-PCL*/ 99 PCL (c), 3 *PPy-b-PCL*/ 97 PCL (d) and 5 *PPy-b-PCL*/ 95 PCL (e).

Table 5. Results of the average distance between the cells and the polymer film.

Sample	Results
1 PPy- <i>b</i> -PCL/ 99 PCL	Without cytotoxicity
3 PPy- <i>b</i> -PCL/ 97 PCL	Without cytotoxicity
5 PPy- <i>b</i> -PCL/ 95 PCL	Without cytotoxicity

Similar to the negative control, the cells proliferated adequately in the wells. Conversely, cells cultured with the standard toxic polymer (positive control) exhibited a spherical shape and detached from the culture dish surface. The micrograph images enabled the measurement of the distance between viable cells and the polymer films. These results were compared with reference values (Table 1) to ascertain the toxicity levels of the samples (Table 5), which demonstrated no toxic effects on cells. PCL is described as a non-toxic polymer in the literature^[10] and PPy exhibits low toxicity^[46]. Therefore, the results suggest that the addition of PPy-*b*-PCL to PCL does not alter its cytotoxicity. This finding aligns with other studies in the literature, indicating that the addition of PPy does not modify the cytotoxicity of the material^[23,47].

4. Conclusions

In this research, the compatibility of PPy-*b*-PCL/PCL blends was investigated using FTIR and Raman spectroscopy, micro-Raman imaging, and TGA analysis. The results from these methods indicated that PCL and PPy-*b*-PCL form compatible blends. Spectroscopic analysis revealed that this compatibility arises from specific interactions between the carboxylic group of PCL and the amine group of PPy-*b*-PCL, as well as between the pyrrole ring of PPy-*b*-PCL and the CH₂ group of PCL. Micro-Raman imaging demonstrated homogeneity in the surface morphology of the polymer blends. Additionally, TGA analysis indicated that the formation of these polymer blends enhances the thermal stability of the material. Importantly, the results showed that the addition of PPy-*b*-PCL does not affect cytotoxicity to bovine fibroblasts, suggesting their biocompatibility and potential use in cattle veterinary devices.

5. Author's Contribution

- **Conceptualization** – Nelson Luis Gonçalves Dias de Souza; Humberto de Mello Brandão; Luiz Fernando Cappa de Oliveira.
- **Data curation** – Nelson Luis Gonçalves Dias de Souza.
- **Formal analysis** – Nelson Luis Gonçalves Dias de Souza; Humberto de Mello Brandão; Luiz Fernando Cappa de Oliveira.
- **Funding acquisition** – Luiz Fernando Cappa de Oliveira.
- **Investigation** – Nelson Luis Gonçalves Dias de Souza; Michele Munk Pereira.

- **Methodology** – Nelson Luis Gonçalves Dias de Souza; Michele Munk Pereira; Humberto de Mello Brandão; Luiz Fernando Cappa de Oliveira.
- **Project administration** – Luiz Fernando Cappa de Oliveira.
- **Resources** – Humberto de Mello Brandão; Luiz Fernando Cappa de Oliveira.
- **Software** – NA.
- **Supervision** – Humberto de Mello Brandão; Luiz Fernando Cappa de Oliveira.
- **Validation** – NA.
- **Visualization** – Nelson Luis Gonçalves Dias de Souza; Grasielle Soares Cavallini; Tiago Teixeira Alves.
- **Writing – original draft** – Nelson Luis Gonçalves Dias de Souza; Grasielle Soares Cavallini; Tiago Teixeira Alves.
- **Writing – review & editing** – Nelson Luis Gonçalves Dias de Souza; Grasielle Soares Cavallini; Tiago Teixeira Alves; Michele Munk Pereira; Humberto de Mello Brandão; Luiz Fernando Cappa de Oliveira.

6. Acknowledgements

The authors wish to thank the Brazilian Agencies National Council of Technological and Scientific Development (CNPq), Coordination of Superior Level Staff Improvement (CAPES), Pro-Rectorate of Research and Graduate Graduation (Federal University of Tocantins – UFT), Federal University of Juiz de Fora, Tocantins Research Support Foundation (FAPT) and Foundation for Research Support of the State of Minas Gerais (FAPEMIG).

7. References

1. Souza, N. L. G. D., Brandão, H. M., & Oliveira, L. F. C. (2014). Chitosan and poly(methyl methacrylate-co-butyl methacrylate) bioblends: a compatibility study. *Polymer-Plastics Technology and Engineering*, 53(4), 319-326. <http://dx.doi.org/10.1080/03602559.2013.844240>.
2. Dasan, K. P., & Rekha, C. (2012). Polymer blend microspheres for controlled drug release: the techniques for preparation and characterization: a review article. *Current Drug Delivery*, 9(6), 588-595. <http://dx.doi.org/10.2174/156720112803529783>. PMID:22780912.
3. Reddy, K. S., Prabhakar, M. N., Babu, P. K., Venkatesulu, G., Rao, U. S. K., Rao, K. C., & Subha, M. C. S. (2012). Miscibility studies of hydroxypropyl cellulose/poly(ethylene glycol) in dilute solutions and solid state. *International Journal of Carbohydrate Chemistry*, 2012, 906389. <http://dx.doi.org/10.1155/2012/906389>.
4. Aid, S., Eddhahak, A., Ortega, Z., Froelich, D., & Tcharkhtchi, A. (2017). Experimental study of the miscibility of ABS/PC polymer blends and investigation of the processing effect. *Journal of Applied Polymer Science*, 134(25), 44975. <http://dx.doi.org/10.1002/app.44975>.
5. Arribada, R. G., Behar-Cohen, F., Barros, A. L. B., & Silva-Cunha, A. (2022). The use of polymer blends in the treatment of ocular diseases. *Pharmaceutics*, 14(7), 1431. <http://dx.doi.org/10.3390/pharmaceutics14071431>. PMID:35890326.

6. Robeson, L. (2014). Historical perspective of advances in the science and technology of polymer blends. *Polymers*, 6(5), 1251-1265. <http://dx.doi.org/10.3390/polym6051251>.
7. Maitz, M. F. (2015). Applications of synthetic polymers in clinical medicine. *Biosurface and Biotribology*, 1(3), 161-176. <http://dx.doi.org/10.1016/j.bsbt.2015.08.002>.
8. Tekade, R. K. (Ed.). (2019). *Basic fundamentals of drug delivery*. London: Academic Press.
9. Li, W., Zhou, J., & Xu, Y. (2015). Study of the in vitro cytotoxicity testing of medical devices. *Biomedical Reports*, 3(5), 617-620. <http://dx.doi.org/10.3892/br.2015.481>. PMID:26405534.
10. Souza, N. L. G. D., Munk, M., Brandão, H. M., & Oliveira, L. F. C. (2017). Cytotoxicity and compatibility of polymeric blend: evaluation of the cytotoxicity in fibroblast bovine cells and compatibility of Poly(ϵ -Caprolactone)/Poly(Methyl Methacrylate-co-Butyl Methacrylate) blend films. *Polymer-Plastics Technology and Engineering*, 56(10), 1076-1083. <http://dx.doi.org/10.1080/03602559.2016.1253735>.
11. Pereira, M. M., Raposo, N. R. B., Brayner, R., Teixeira, E. M., Oliveira, V., Quintão, C. C. R., Camargo, L. S. A., Mattoso, L. H. C., & Brandão, H. M. (2013). Cytotoxicity and expression of genes involved in the cellular stress response and apoptosis in mammalian fibroblast exposed to cotton cellulose nanofibers. *Nanotechnology*, 24(7), 075103. <http://dx.doi.org/10.1088/0957-4484/24/7/075103>. PMID:23358497.
12. Liu, Z.-H., Li, Y., Zhang, C.-J., Zhang, Y.-Y., Cao, X.-H., & Zhang, X.-H. (2020). Synthesis of high-molecular-weight poly(ϵ -caprolactone) via heterogeneous zinc-cobalt(III) double metal cyanide complex. *Giant*, 3, 100030. <http://dx.doi.org/10.1016/j.giant.2020.100030>.
13. Arcana, I. M., Bundjali, B., Yudistira, I., Jariah, B., & Sukria, L. (2007). Study on properties of polymer blends from polypropylene with polycaprolactone and their biodegradability. *Polymer Journal*, 39(12), 1337-1344. <http://dx.doi.org/10.1295/polymj.PJ2006250>.
14. Martin, D. P., & Williams, S. F. (2003). Medical applications of poly-4-hydroxybutyrate: a strong flexible absorbable biomaterial. *Biochemical Engineering Journal*, 16(2), 97-105. [http://dx.doi.org/10.1016/S1369-703X\(03\)00040-8](http://dx.doi.org/10.1016/S1369-703X(03)00040-8).
15. Malikmammadov, E., Tanir, T. E., Kiziltay, A., Hasirci, V., & Hasirci, N. (2018). PCL and PCL-based materials in biomedical applications. *Journal of Biomaterials Science. Polymer Edition*, 29(7-9), 863-893. <http://dx.doi.org/10.1080/09205063.2017.1394711>. PMID:29053081.
16. Talebi, A., Labbaf, S., & Karimzadeh, F. (2020). Polycaprolactone-chitosan-polyppyrrrole conductive biocomposite nanofibrous scaffold for biomedical applications. *Polymer Composites*, 41(2), 645-652. <http://dx.doi.org/10.1002/pc.25395>.
17. Zhang, Z., Roy, R., Dugré, F. J., Tessier, D., & Dao, L. H. (2001). In vitro biocompatibility study of electrically conductive polypyrrrole-coated polyester fabrics. *Journal of Biomedical Materials Research*, 57(1), 63-71. [http://dx.doi.org/10.1002/1097-4636\(200110\)57:1<63::AID-JBM1142>3.0.CO;2-L](http://dx.doi.org/10.1002/1097-4636(200110)57:1<63::AID-JBM1142>3.0.CO;2-L). PMID:11416850.
18. Ramanaviciene, A., Kausaitė, A., Tautkus, S., & Ramanavicius, A. (2007). Biocompatibility of polypyrrrole particles: an in-vivo study in mice. *The Journal of Pharmacy and Pharmacology*, 59(2), 311-315. <http://dx.doi.org/10.1211/jpp.59.2.0017>. PMID:17270084.
19. Hardy, J. G., Lee, J. Y., & Schmidt, C. E. (2013). Biomimetic conducting polymer-based tissue scaffolds. *Current Opinion in Biotechnology*, 24(5), 847-854. <http://dx.doi.org/10.1016/j.copbio.2013.03.011>. PMID:23578463.
20. Razavi, M. (2017). *Biomaterials for tissue engineering*. London: Bentham Science Publishers.
21. Rocha, M. F. B., Aguiar, M. F., Vinhas, G. M., Melo, C. P., Morelli, C. L., & Alves, K. G. B. (2023). Preparation and characterization of PLA/polypyrrrole blends with antibacterial properties. *Materials Research*, 26(Suppl. 1), e20230045. <http://dx.doi.org/10.1590/1980-5373-mr-2023-0045>.
22. Yang, S., Jang, L., Kim, S., Yang, J., Yang, K., Cho, S.-W., & Lee, J. Y. (2016). Polypyrrrole/alginate hybrid hydrogels: electrically conductive and soft biomaterials for human mesenchymal stem cell culture and potential neural tissue engineering applications. *Macromolecular Bioscience*, 16(11), 1653-1661. <http://dx.doi.org/10.1002/mabi.201600148>. PMID:27455895.
23. Vijayavenkataraman, S., Vialli, N., Fuh, J. Y. H., & Lu, W. F. (2019). Conductive collagen/polypyrrrole-b-polycaprolactone hydrogel for bioprinting of neural tissue constructs. *International Journal of Bioprinting*, 5(1), 229. <http://dx.doi.org/10.18063/ijb.v5i1.1.229>.
24. Zhu, G., Wang, F., Xu, K., Gao, Q., & Liu, Y. (2013). Study on properties of poly(vinyl alcohol)/polyacrylonitrile blend film. *Polimeros*, 23(2), 146-151. <http://dx.doi.org/10.4322/polimeros.2013.076>.
25. Rojanapitayakorn, P., Thongyai, S., Higgins, J. S., & Clarke, N. (2001). Effects of sample preparation method on mixing and phase separation in binary polymer blends. *Polymer*, 42(8), 3475-3487. [http://dx.doi.org/10.1016/S0032-3861\(00\)00783-7](http://dx.doi.org/10.1016/S0032-3861(00)00783-7).
26. Leite, A. M. D., Araújo, E. M., Lira, H. L., Barbosa, R., & Ito, E. N. (2009). Obtenção de membranas microporosas a partir de manocompósitos de poliamida 6/argila nacional. Parte 1: influência da presença da argila na morfologia das membranas. *Polímeros*, 19(4), 271-277. <http://dx.doi.org/10.1590/S0104-14282009000400005>.
27. Souza, N. L. G. D., Munk, M., Brandão, H. M., & Oliveira, L. F. C. (2018). Functionalization of poly(epichlorohydrin) using sodium hydrogen squarate: cytotoxicity and compatibility in blends with chitosan. *Polymer Bulletin*, 75(10), 4627-4639. <http://dx.doi.org/10.1007/s00289-018-2290-5>.
28. Arjomandi, J., Shah, A.-U.-H. A., Bilal, S., Van Hoang, H., & Holze, R. (2011). In situ Raman and UV-vis spectroscopic studies of polypyrrrole and poly(pyrrole-2,6-dimethyl- β -cyclodextrin). *Spectrochimica Acta. Part A: Molecular and Biomolecular Spectroscopy*, 78(1), 1-6. <http://dx.doi.org/10.1016/j.saa.2009.12.026>. PMID:21111671.
29. Ourari, A., Aggoun, D., & Ouahab, L. (2014). Poly(pyrrole) films efficiently electrodeposited using new monomers derived from 3-bromopropyl-N-pyrrol and dihydroxyacetophenone: electrocatalytic reduction ability towards bromocyclopentane. *Colloids and Surfaces. A, Physicochemical and Engineering Aspects*, 446, 190-198. <http://dx.doi.org/10.1016/j.colsurfa.2014.01.047>.
30. Misra, R. M., Agarwal, R., Tandon, P., & Gupta, V. D. (2004). Phonon dispersion and heat capacity in poly(ϵ -caprolactone). *European Polymer Journal*, 40(8), 1787-1798. <http://dx.doi.org/10.1016/j.eurpolymj.2004.04.022>.
31. Hou, Y., Zhang, L., Chen, L. Y., Liu, P., Hirata, A., & Chen, M. W. (2014). Raman characterization of pseudocapacitive behavior of polypyrrrole on nanoporous gold. *Physical Chemistry Chemical Physics*, 16(8), 3523-3528. <http://dx.doi.org/10.1039/c3cp54497d>. PMID:24441648.
32. Nartker, S., Hassan, M., & Stogsdill, M. (2015). Electrospun cellulose nitrate and polycaprolactone blended nanofibers. *Materials Research Express*, 2(3), 035401. <http://dx.doi.org/10.1088/2053-1591/2/3/035401>.
33. Abdelrazek, E. M., Hezma, A. M., El-khodary, A., & Elzayat, A. M. (2016). Spectroscopic studies and thermal properties of PCL/PMMA biopolymer blend. *Egyptian Journal of Basic and Applied Sciences*, 3(1), 10-15. <http://dx.doi.org/10.1016/j.ejbas.2015.06.001>.

34. Kołodziej, A., Długoń, E., Świątek, M., Ziąbka, M., Dawiec, E., Gubernat, M., Michalec, M., & Weselucha-Birczyńska, A. (2021). A Raman spectroscopic analysis of polymer membranes with graphene oxide and reduced graphene oxide. *Journal of Composites Science*, 5(1), 20. <http://dx.doi.org/10.3390/jcs5010020>.
35. Phillipson, K., Hay, J. N., & Jenkins, M. J. (2014). Thermal analysis FTIR spectroscopy of poly(ϵ -caprolactone). *Thermochimica Acta*, 595, 74-82. <http://dx.doi.org/10.1016/j.tca.2014.08.027>.
36. Ángeles Corres, M., Mugica, A., Carrasco, P. M., & Milagros Cortázar, M. (2006). Effect of crystallization on morphology-conductivity relationship in polypyrrole/poly(ϵ -caprolactone) blends. *Polymer*, 47(19), 6759-6764. <http://dx.doi.org/10.1016/j.polymer.2006.07.042>.
37. Basavaraja, C., Kim, W. J., Kim, D. G., & Huh, D. S. (2011). Synthesis and characterization of soluble polypyrrole-poly(ϵ -caprolactone) polymer blends with improved electrical conductivities. *Materials Chemistry and Physics*, 129(3), 787-793. <http://dx.doi.org/10.1016/j.matchemphys.2011.05.057>.
38. Mitsutake, H., Poppi, R. J., & Breitreit, M. C. (2019). Raman imaging spectroscopy: history, fundamentals and current scenario of the technique. *Journal of the Brazilian Chemical Society*, 30(11), 2243-2258. <http://dx.doi.org/10.21577/0103-5053.20190116>.
39. Shirahase, T., Komatsu, Y., Tominaga, Y., Asai, S., & Sumita, M. (2006). Miscibility and hydrolytic degradation in alkaline solution of poly(L-lactide) and poly(methyl methacrylate) blends. *Polymer*, 47(13), 4839-4844. <http://dx.doi.org/10.1016/j.polymer.2006.04.012>.
40. Sivalingam, G., & Madras, G. (2003). Thermal degradation of poly(ϵ -caprolactone). *Polymer Degradation & Stability*, 80(1), 11-16. [http://dx.doi.org/10.1016/S0141-3910\(02\)00376-2](http://dx.doi.org/10.1016/S0141-3910(02)00376-2).
41. Choo, K., Ching, Y. C., Chuah, C. H., Julai, S., & Liou, N.-S. (2016). Preparation and characterization of polyvinyl alcohol-chitosan composite films reinforced with cellulose nanofiber. *Materials*, 9(8), 644. <http://dx.doi.org/10.3390/ma9080644>. PMID:28773763.
42. Marangoni Júnior, L., Rodrigues, P. R., Silva, R. G., Vieira, R. P., & Alves, R. M. V. (2021). Sustainable packaging films composed of sodium alginate and hydrolyzed collagen: preparation and characterization. *Food and Bioprocess Technology*, 14(12), 2336-2346. <http://dx.doi.org/10.1007/s11947-021-02727-7>.
43. Zhang, M., Ding, C., Chen, L., & Huang, L. (2013). The preparation of cellulose/collagen composite films using 1-ethyl-3-methylimidazolium acetate as a solvent. *BioResources*, 9(1), 756-771. <http://dx.doi.org/10.15376/biores.9.1.756-771>.
44. Yang, M. Y., & Rajamahendran, R. (2000). Morphological and biochemical identification of apoptosis in small, medium, and large bovine follicles and the effects of follicle-stimulating hormone and insulin-like growth factor-I on spontaneous apoptosis in cultured bovine granulosa cells. *Biology of Reproduction*, 62(5), 1209-1217. <http://dx.doi.org/10.1095/biolreprod62.5.1209>. PMID:10775168.
45. Rello, S., Stockert, J. C., Moreno, V., Gámez, A., Pacheco, M., Juarranz, A., Cañete, M., & Villanueva, A. (2005). Morphological criteria to distinguish cell death induced by apoptotic and necrotic treatments. *Apoptosis*, 10(1), 201-208. <http://dx.doi.org/10.1007/s10495-005-6075-6>. PMID:15711936.
46. Manzari-Tavakoli, A., Tarasi, R., Sedghi, R., Moghimi, A., & Niknejad, H. (2020). Fabrication of nanochitosan incorporated polypyrrole/alginate conducting scaffold for neural tissue engineering. *Scientific Reports*, 10(1), 22012. <http://dx.doi.org/10.1038/s41598-020-78650-2>. PMID:33328579.
47. Ferreira, C. L., Valente, C. A., Zanini, M. L., Sgarioni, B., Tondo, P. H. F., Chagastelles, P. C., Braga, J., Campos, M. M., Malmonge, J. A., & Basso, N. R. S. (2019). Biocompatible PCL/PLGA/polypyrrole composites for regenerating nerves. *Macromolecular Symposia*, 383(1), 1800028. <http://dx.doi.org/10.1002/masy.201800028>.

Received: Aug. 29, 2023

Revised: Jan. 25, 2024

Accepted: Jan. 30, 2024